22 Wheelset

22.1 General Information

The wheelset is an IDE of dimension 17 which shows some typical properties of simulation problems in contact mechanics, i.e., friction, contact conditions, stiffness, etc.. This problem is originally described by an index 3 IDE with additional index 1 equations, but can be reduced to index 2. Test results are based on the index-2 formulation. This problem was contributed by Bernd Simeon, Claus Führer, Peter Rentrop, Nov. 1995. Comments to `simeon@ma.tum.de` or `Claus.Fuhrer@na.lu.se`. See also [SFR91].

The software part of the problem is in the file wheel.f available at [MM08].

22.2 Mathematical description of the problem

The index 3 formulation of the wheelset problem reads

$$\dot{p} = v, \tag{II.22.1}$$

$$M(p)\begin{pmatrix} \dot{v} \\ \dot{\beta} \end{pmatrix} = \begin{pmatrix} f(u) - (\partial g_1(p,q)/\partial p)^{\mathrm{T}} C\lambda \\ d(u) \end{pmatrix}, \tag{II.22.2}$$

$$0 = g_1(p,q), \tag{II.22.3}$$

$$0 = g_2(p,q), \tag{II.22.4}$$

where $u := (p, v, \beta, q, \lambda)^{\mathrm{T}} \in \mathbb{R}^{17}$, $p, v \in \mathbb{R}^5$, $\beta \in \mathbb{R}$, $q \in \mathbb{R}^4$, $\lambda \in \mathbb{R}^2$ and C is a scalar constant. Furthermore, $M : \mathbb{R}^5 \to \mathbb{R}^6 \times \mathbb{R}^6$, $f : \mathbb{R}^{17} \to \mathbb{R}^5$, $d : \mathbb{R}^{17} \to \mathbb{R}$, $g_1 : \mathbb{R}^9 \to \mathbb{R}^2$ and $g_2 : \mathbb{R}^9 \to \mathbb{R}^4$. The integration interval is from 0 to 10 [s].

For the index 2 formulation of the problem (II.22.3) is replaced by

$$0 = (\partial g_1(p,q)/\partial p)\, v. \tag{II.22.5}$$

The non-zero components of the consistent initial values $u(0) := u_0$ and $u'(0) := u'_0$ are given by

$u_{0,1}$	$0.1494100000000000 \cdot 10^{-2}$	$u_{0,12}$	$7.4122380357667139 \cdot 10^{-6}$
$u_{0,2}$	$0.4008900000000000 \cdot 10^{-6}$	$u_{0,13}$	0.1521364296121248
$u_{0,3}$	$0.1124100000000000 \cdot 10^{-5}$	$u_{0,14}$	$7.5634406395172940 \cdot 10^{-6}$
$u_{0,4}$	$-0.2857300000000000 \cdot 10^{-3}$	$u_{0,15}$	0.1490635714733819
$u_{0,5}$	$0.2645900000000000 \cdot 10^{-3}$	$u_{0,16}$	$-0.8359300000000000 \cdot 10^{-2}$
		$u_{0,17}$	$-0.7414400000000000 \cdot 10^{-2}$

$u'_{0,6}$	-1.9752588940112850	$u'_{0,9}$	-5.5333628217315490
$u'_{0,7}$	$-1.0898297102811276 \cdot 10^{-3}$	$u'_{0,10}$	-0.3487021489546511
$u'_{0,8}$	$7.8855083626142589 \cdot 10^{-2}$	$u'_{0,11}$	-2.1329687243809270

The other components of u_0 and u'_0 are zero. For the index 3 formulation, the index of variables p, v, β, q and λ equals 1, 2, 2, 1 and 3. For the index 2 problem, these numbers read 1, 1, 1, 1 and 2.

The equations are given in detail in the next subsections, in which some references to the origin of the problem, treated in §22.3, are already given. Table II.22.1 lists all problem parameters.

22.2.1 Differential equations

The position coordinates p are defined as

$$p := \begin{pmatrix} x \\ y \\ z \\ \theta \\ \varphi \end{pmatrix} \qquad \begin{array}{l} \text{lateral displacement} \\ \text{vertical displacement} \\ \text{longitudinal displacement} \\ \text{yaw angle} \\ \text{roll angle} \end{array}$$

and the contact variables as $q^{\mathrm{T}} := (\ \psi_L \quad \xi_L \quad \psi_R \quad \xi_R\ )$ with

$$\begin{aligned} \xi_{L|R} &:= \text{coordinate of the contact point left/right,} \\ \psi_{L|R} &:= \text{shift angle left/right.} \end{aligned}$$

The first three equations in (II.22.2) yield the momentum equations:

$$\begin{aligned} m_R\,\ddot{x} &= m_R\left(2\,v_0\,\kappa\,\cos\alpha\,\dot{z} + v_0^2\,\kappa\,\cos\alpha\,(1+\kappa\,(x\cos\alpha - y\sin\alpha))\right) \\ &\quad + T_{L_1} + T_{R_1} + Q_1 - m_R\,\tilde{g}\,\sin\alpha - b_{1,1}\,\lambda_1 - b_{1,2}\,\lambda_2 - 2\,c_x\,x\,, \\ m_R\,\ddot{y} &= -m_R\left(2\,v_0\,\kappa\,\sin\alpha\,\dot{z} + v_0^2\,\kappa\,\sin\alpha\,(1+\kappa\,(x\cos\alpha - y\sin\alpha))\right) \\ &\quad + T_{L_2} + T_{R_2} + Q_2 - m_R\,\tilde{g}\,\cos\alpha - b_{2,1}\,\lambda_1 - b_{2,2}\,\lambda_2\,, \\ m_R\,\ddot{z} &= m_R\left(-2\,v_0\,\kappa\,(\dot{x}\cos\alpha - \dot{y}\sin\alpha) + v_0^2\,\kappa^2\,z\right) \\ &\quad + T_{L_3} + T_{R_3} + Q_3 + F_A - b_{3,1}\,\lambda_1 - b_{3,2}\,\lambda_2\,, \end{aligned}$$

where $b_{i,j}$ denotes the (i,j) element of the constraint Jacobian $\partial g_1(p,q)/\partial p$. The next three equations yield the spin equations:

$$\begin{aligned} I_2\,\ddot{\theta}\,\cos\varphi &= -\dot{\theta}\,\dot{\varphi}\sin\varphi + v_0\,\kappa\Big(\,\dot{\varphi}(\sin\alpha\cos\theta\cos\varphi + \cos\alpha\sin\varphi) - \dot{\theta}\sin\alpha\sin\theta\sin\varphi\Big) \\ &\quad -I_1\,(\omega_0+\beta)\,(\dot{\varphi} - v_0\kappa\sin\theta\sin\alpha) \\ &\quad -(I_1 - I_2)\left(\dot{\theta}\,\sin\varphi - v_0\,\kappa\,(\cos\theta\cos\varphi\sin\alpha + \sin\varphi\cos\alpha)\right) \\ &\qquad\qquad \left(\dot{\varphi} - v_0\,\kappa\,\sin\alpha\sin\theta\right) \\ &\quad +\Big[\,-(\xi_L\sin\theta + R(\xi_L)\sin\psi_L\cos\theta\cos\varphi)\,T_{L_1} \\ &\qquad -R(\xi_L)\sin\psi_L\sin\varphi\,T_{L_2} \\ &\qquad +(-\xi_L\cos\theta + R(\xi_L)\sin\psi_L\sin\theta\cos\varphi)\,T_{L_3}\Big] \\ &\quad +\Big[\quad \text{corresponding terms of the right side} \quad\Big] \\ &\quad -\cos\theta\,\sin\varphi\,M_1 + \cos\varphi\,M_2 + \sin\theta\,\sin\varphi\,M_3 - b_{4,1}\,\lambda_1 - b_{4,2}\,\lambda_2\,, \\ I_2\,\ddot{\varphi} &= I_2\,\dot{\theta}\,v_0\,\kappa\,\sin\alpha\,\cos\theta \\ &\quad +I_1\,(\omega_0+\beta)\left(\dot{\theta}\cos\varphi + v_0\,\kappa\,(\cos\theta\sin\varphi\sin\alpha - \cos\varphi\cos\alpha)\right) \\ &\quad +(I_1 - I_2)\Big(\dot{\theta}\,\sin\varphi - v_0\,\kappa(\cos\theta\cos\varphi\sin\alpha + \sin\varphi\cos\alpha)\Big) \\ &\qquad\qquad \Big(\dot{\theta}\,\cos\varphi + v_0\,\kappa(\cos\theta\sin\varphi\sin\alpha - \cos\varphi\cos\alpha)\Big) \\ &\quad +\Big[\,-(\xi_L\cos\theta\sin\varphi - R(\xi_L)\cos\psi_L\cos\theta\cos\varphi)\,T_{L_1} \\ &\qquad +(\xi_L\cos\varphi + R(\xi_L)\cos\psi_L\sin\varphi)\,T_{L_2} \\ &\qquad +(\xi_L\sin\theta\sin\varphi - R(\xi_L)\cos\psi_L\sin\theta\cos\varphi)\,T_{L_3}\Big] \\ &\quad +\Big[\quad \text{corresponding terms of the right side} \quad\Big] \\ &\quad +\sin\theta\,M_1 + \cos\theta\,M_3 - b_{5,1}\,\lambda_1 - b_{5,2}\,\lambda_2\,, \end{aligned}$$

$$
\begin{aligned}
I_1\,(\dot\beta\,+\,\ddot\theta\,\sin\varphi) \;=\;& \dot\theta\,\dot\varphi\cos\varphi - v_0\,\kappa\,(\dot\varphi(\cos\alpha\cos\varphi - \sin\alpha\cos\theta\sin\varphi) - \dot\theta\sin\alpha\sin\theta\cos\varphi)\\
&+\Big[-R(\xi_L)\,(\cos\psi_L\sin\theta + \sin\psi_L\cos\theta\sin\varphi)\,T_{L_1}\\
&\quad +R(\xi_L)\,\sin\psi_L\,\cos\varphi\,T_{L_2}\\
&\quad -R(\xi_L)\,(\cos\psi_L\cos\theta - \sin\psi_L\sin\theta\sin\varphi)\,T_{L_3}\Big]\\
&+\Big[\quad\text{corresponding terms of the right side}\quad\Big]\\
&+\cos\theta\,\cos\varphi\,M_1 + \sin\varphi\,M_2 - \sin\theta\,\cos\varphi\,M_3 + L_A\,.
\end{aligned}
$$

The forces Q and moments M of the wagon body satisfy the following equations:

$$
\begin{aligned}
Q_1 &= \tfrac{m_A\,\bar g}{\cos\alpha}\left(\tfrac{v_0^2\,\kappa}{\bar g} - \tan\alpha\right) && \text{(lateral force)},\\
Q_2 &= -m_A\,\tilde g\,\cos\alpha\,\left(\tfrac{v_0^2\,\kappa}{\bar g}\,\tan\alpha + 1\right) && \text{(vertical force)},\\
Q_3 &= -2\,c_z\,z && \text{(longitudinal force)},\\
M_1 &= 0\\
M_2 &= Q_3\,x_l && \text{(yaw moment)},\\
M_3 &= -h_A\,Q_1 && \text{(roll moment)},\\
0 &= \cos\theta\,M_1 - \sin\theta\,M_3 && \text{(no pitch moment)}.
\end{aligned}
$$

The creep forces $T_{L_{1,2,3}}$ and $T_{R_{1,2,3}}$ of the left and right contact point are obtained via the transformation

$$
\begin{pmatrix} T_{L|R_1}\\ T_{L|R_2}\\ T_{L|R_3}\end{pmatrix} = \begin{pmatrix} \sin\theta & \cos\theta\cos\Delta_{L|R} & \mp\cos\theta\sin\Delta_{L|R}\\ 0 & \pm\sin\Delta_{L|R} & \cos\Delta_{L|R}\\ \cos\theta & -\sin\theta\cos\Delta_{L|R} & \pm\sin\theta\sin\Delta_{L|R}\end{pmatrix}\begin{pmatrix} T_{1_{L|R}}\\ T_{2_{L|R}}\\ 0\end{pmatrix},
$$

where $T_{1_{L|R}}$ and $T_{2_{L|R}}$ denote the creep forces with respect to the local reference frame of the contact point and $\pm$ stands for the left and right side, respectively. The creep forces are approximated by

$$
\begin{aligned}
T_{1_{L|R}} &:= -\mu N_{L|R}\tanh\left(\frac{GC_{11}c^2}{\mu N_{L|R}}\nu_1\right),\\
T_{2_{L|R}} &:= -\mu N_{L|R}\tanh\left(\frac{GC_{22}c^2}{\mu N_{L|R}}\nu_2 + \frac{GC_{23}c^3}{\mu N_{L|R}}\varphi_3\right),
\end{aligned}
$$

and corrected by

$$
\begin{aligned}
&\text{if}\quad T_1^2 + T_2^2 > (\mu N)^2\,,\quad \text{then}\\
&\tilde T_1 := \frac{T_1}{\sqrt{T_1^2+T_2^2}}\,\mu N \quad\text{and}\quad \tilde T_2 := \frac{T_2}{\sqrt{T_1^2+T_2^2}}\,\mu N.
\end{aligned}
$$

The constant parameters

$$
\mu, G, C_{11}, C_{22}, C_{23}
$$

(friction coefficient, glide module, Kalker coefficients) are listed in Table II.22.1. For the computation of c, the size of contact ellipse, which uses the parameters σ, $\widehat{G}$ and ϵ, we refer to [Jas87]. For alternative creep force models see also [Jas87].

The normal forces N are given by

$$
\begin{pmatrix} N_L\\ N_R\end{pmatrix} = \gamma\begin{pmatrix} \cos\Delta_R & -\sin\Delta_R\\ -\cos\Delta_L & -\sin\Delta_L\end{pmatrix}\begin{pmatrix} b_{1,1} & b_{1,2}\\ b_{2,1} & b_{2,2}\end{pmatrix}\begin{pmatrix}\lambda_1\\ \lambda_2\end{pmatrix},
$$

where

$$\gamma := \frac{1}{\sin\Delta_L\cos\Delta_R + \sin\Delta_R\cos\Delta_L}\,.$$

Here, $\Delta_{L|R}$ denotes the contact angles and is defined as

$$\begin{aligned}
\tan\Delta_L &= \frac{(R'(\xi_L)\cos\varphi - \sin\varphi\cos\psi_L)\cos\theta + \sin\psi_L\sin\theta}{-R'(\xi_L)\sin\varphi - \cos\psi_L\cos\varphi}\,;\\
\tan\Delta_R &= \frac{(R'(\xi_R)\cos\varphi - \sin\varphi\cos\psi_R)\cos\theta + \sin\psi_R\sin\theta}{+R'(\xi_R)\sin\varphi + \cos\psi_R\cos\varphi}\,.
\end{aligned}$$

For the creepages we have the relations

$$\begin{aligned}
\nu_1 &= \frac{1}{v_{roll}}\left(\sin\theta v_{r1} + \cos\theta v_{r3}\right)\\
\nu_2 &= \frac{1}{v_{roll}}\left(\cos\theta\cos\Delta_{L|R}v_{r1} \pm \sin\Delta_{L|R}v_{r2} - \sin\theta\cos\Delta_{L|R}v_{r3}\right)\\
\varphi_3 &= \frac{1}{v_{roll}}\Big(\mp\sin\Delta_{L|R}(\omega+\beta-v_0\,\kappa\,\sin\alpha) + \cos\Delta_{L|R}(\dot\theta - v_0\,\kappa\cos\alpha)\Big)
\end{aligned}$$

where $v_{r1,2,3}$ (relative velocity at the contact point) and v_{roll} (rolling velocity) are given by (correspondingly for the right side)

$$\begin{aligned}
v_{r1} &= \dot x - \dot\theta(R(\xi_L)(\sin\theta\sin\varphi\cos\psi_L + \cos\theta\sin\psi_L) + \xi_L\sin\theta\cos\varphi)\\
&\quad -\dot\varphi\cos\theta(\xi_L\sin\varphi - R(\xi_L)\cos\varphi\cos\psi_L)\\
&\quad +(\omega_0+\beta)R(\xi_L)(-\sin\theta\cos\psi_L - \sin\varphi\cos\theta\sin\psi_L)\\
&\quad +v_0\kappa\cos\alpha(R(\xi_L)(\sin\theta\sin\varphi\cos\psi_L + \cos\theta\sin\psi_L) + \xi_L\sin\theta\cos\varphi - z),\\
v_{r2} &= \dot y + \dot\varphi(\xi_L\cos\varphi + R(\xi_L)\sin\varphi\cos\psi_L) + (\omega_0+\beta)R(\xi_L)\cos\varphi\sin\psi_L\\
&\quad +v_0\kappa\sin\alpha(z - \xi_L\sin\theta\cos\varphi - R(\xi_L)(\sin\theta\sin\varphi\cos\psi_L + \cos\theta\sin\psi_L)),\\
v_{r3} &= \dot z + v_0 + v_0\kappa(x\cos\alpha - y\sin\alpha)\\
&\quad -\dot\theta(\xi_L\cos\theta\cos\varphi + R(\xi_L)(\cos\theta\sin\varphi\cos\psi_L - \sin\theta\sin\psi_L))\\
&\quad +\dot\varphi\sin\theta(\xi_L\sin\varphi - R(\xi_L)\cos\varphi\cos\psi_L)\\
&\quad +(\omega+\beta)R(\xi_L)(\sin\theta\sin\varphi\sin\psi_L - \cos\theta\cos\psi_L)\\
&\quad -v_0\kappa\sin\alpha(\xi_L\sin\varphi - R(\xi_L)\cos\varphi\cos\psi_L)\\
&\quad +v_0\cos\alpha(\xi_L\cos\theta\cos\varphi + R(\xi_L)(\cos\theta\sin\varphi\cos\psi_L - \sin\theta\sin\psi_L)),
\end{aligned}$$

and

$$v_{roll} = \frac{1}{2}\left\|\begin{pmatrix} -2\dot x + 2v_0\kappa z\cos\alpha\\ -2\dot y - 2v_0\kappa z\sin\alpha\\ -2\dot z - 2v_0 - 2v_0\kappa(x\cos\alpha - y\sin\alpha)\end{pmatrix} + \begin{pmatrix} v_{r1}\\ v_{r2}\\ v_{r3}\end{pmatrix}\right\|_2\,.$$

22.2.2 Constraints

The constraints (II.22.3) read

$$\begin{pmatrix} G(\hat\xi_L) - y - \xi_L\sin\varphi + R(\xi_L)\cos\varphi\cos\psi_L\\ G(\hat\xi_R) - y - \xi_R\sin\varphi + R(\xi_R)\cos\varphi\cos\psi_R\end{pmatrix} = 0$$

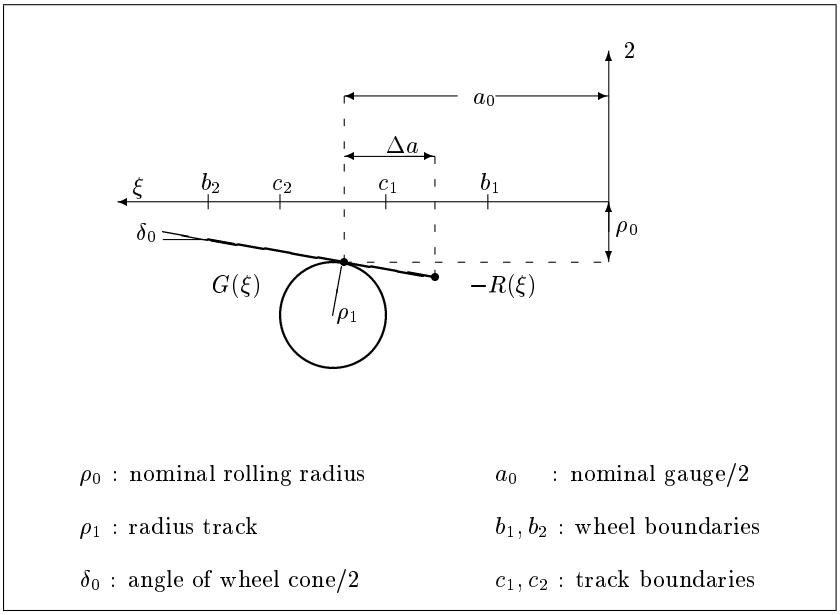

FIGURE II.22.1: *Profile functions (left side).*

with profile functions R (wheel) and G (rail), see Figure II.22.1,

$$R(\xi) \quad = \quad \rho_0 + \tan\delta_0\,(a_0 - |\xi|) \qquad \text{for } a_0 - \Delta a < |\xi| < b_2\,;$$

$$G(\hat{\xi}) \quad = \quad \sqrt{\rho_1^2 - \left(|\hat{\xi}| - a_0 - \rho_1 \sin\delta_0\right)^2} - \rho_0 - \cos\delta_0\,\rho_1 \qquad \text{for } c_1 < |\hat{\xi}| < c_2\,.$$

Here, ξ stands for the left or right coordinate $\xi_{L/R}$, respectively, and $\hat{\xi}$ is defined by

$$\hat{\xi}_{L|R} := x + \xi_{L|R}\cos\theta\cos\varphi + R(\xi_{L|R})\left(\cos\theta\sin\varphi\cos\psi_{L|R} - \sin\theta\sin\psi_{L|R}\right).$$

The constraints (II.22.4) read

$$\begin{aligned} G'(\hat{\xi}_L)\,(R'(\xi_L)\sin\varphi + \cos\varphi\cos\psi_L) + R'(\xi_L)\cos\theta\cos\varphi & \\ -\cos\theta\sin\varphi\cos\psi_L + \sin\theta\sin\psi_L \quad &= \quad 0, \\ R'(\xi_L)\sin\theta\cos\varphi - \sin\theta\sin\varphi\cos\psi_L - \cos\theta\sin\psi_L \quad &= \quad 0, \\ G'(\hat{\xi}_R)\,(R'(\xi_R)\sin\varphi + \cos\varphi\cos\psi_R) + R'(\xi_R)\cos\theta\cos\varphi & \\ -\cos\theta\sin\varphi\cos\psi_R + \sin\theta\sin\psi_R \quad &= \quad 0, \\ R'(\xi_R)\sin\theta\cos\varphi - \sin\theta\sin\varphi\cos\psi_R - \cos\theta\sin\psi_R \quad &= \quad 0, \end{aligned}$$

where $G'(\hat{\xi}_{L|R}) := \frac{\mathrm{d}}{\mathrm{d}\hat{\xi}_{L|R}} G(\hat{\xi}_{L|R})\,, R'(\xi_{L|R}) := \frac{\mathrm{d}}{\mathrm{d}\xi_{L|R}} R(\xi_{L|R})$.

22.3 Origin of the problem

The motion of a simple wheelset on a rail track exhibits a lot of the difficulties which occur in the simulation of contact problems in mechanics. The state space form approach for this class of problems

TABLE II.22.1: *Parameter values according to [Jas90], where a hardware bogie model, scaled 1:4, is investigated.*

Parameter	Meaning	Unit	Value
m_R	mass wheelset	kg	16.08
$\tilde{g}$	gravity constant	m/s^2	9.81
v_0	nominal velocity	m/s	30.0
F_A	propulsion force	N	0
L_A	propulsion moment	kg m^2	0
κ	describes track geometry		0
α	describes track geometry	rad	0
ω_0	nominal angular velocity	1/s	v_0/ρ_0
I_1	lateral moment of inertia	kg m^2	0.0605
I_2	vertical moment of inertia	kg m^2	0.366
m_A	mass of wagon body	kg	0.0
h_A	height of wagon body	m	0.2
c_x	spring constant	N/m	6400.0
c_z	spring constant	N/m	6400.0
x_l	width of wheelset/2	m	0.19
δ_0	cone angle/2	rad	0.0262
ρ_0	nominal radius	m	0.1
a_0	gauge/2	m	0.1506
ρ_1	radius track	m	0.06
μ	friction coefficient		0.12
G	glide module	N/m^2	$7.92 \cdot 10^{10}$
C_{11}	Kalker coefficient		4.72772197
C_{22}	Kalker coefficient		4.27526987
C_{23}	Kalker coefficient		1.97203505
$\widehat{G}$	parameter for computation of contact ellipse		0.7115218
ϵ	parameter for computation of contact ellipse		1.3537956
σ	parameter for computation of contact ellipse		0.28
C	scaling factor for Lagrange multipliers		10^4

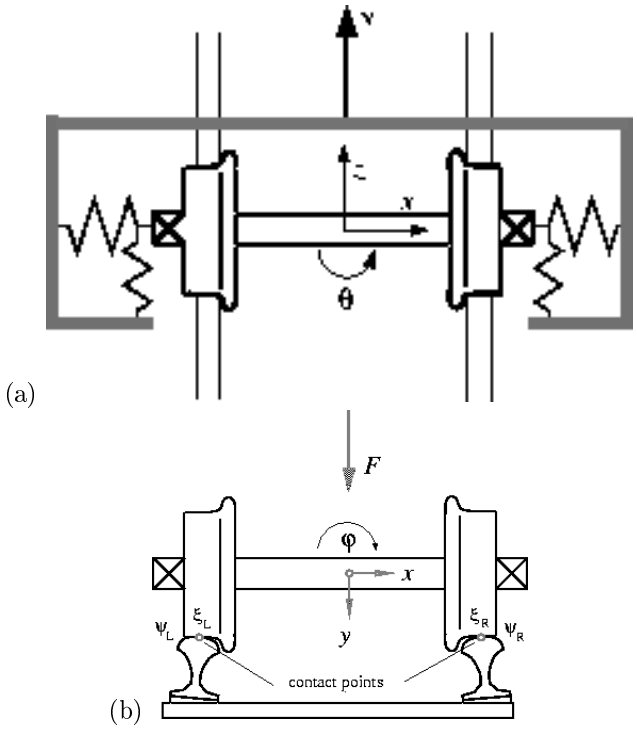

FIGURE II.22.2: *The wheelset and the track. (a) View from above, (b) lateral cross section.*

requires simplifications and table look ups in order to eliminate the nonlinear constraints. The above example provides thus an alternative by using the IDE approach.

Figure II.22.2 shows the mechanical model. The coordinates p denote the displacements and rotations of the wheelset with respect to the reference frame which is centered in the middle of the track. The wheelset is subjected to

- the gravity and centrifugal forces;
- creep forces in the contact points of wheel and rail;
- forces of the wagon body, which is represented by a frame connected to the wheelset via springs and dampers and proceeding with constant speed v_0;
- constraint forces which enforce the contact of wheel and rail on both sides.

We are particularly interested in a complete and correct formulation of the nonlinear constraint equations. An elimination of the constraints without severe simplifications or the introduction of tables for the dependent variables is impossible. In this example thus a reduction to state space form involves various obstacles, whereas the IDE formulation is straightforward.

Equations (II.22.1)–(II.22.2) stand for the kinematic and dynamic equations with positive definite mass matrix $M(p)$. By means of the profile functions R and G which describe the cross sections of wheel and rail depending on the contact points we first express the constraint equations as $0 = g_1$, see Figure II.22.3. These constraints are of index 3 and enforce that the contact points of wheel and rail coincide on both sides. Additionally, we have to guarantee that wheel and rail do not intersect, which is accomplished by the conditions $0 = g_2$. Note that $\partial g_2/\partial q$ is regular, which means that we can apply formally the implicit function theorem to eliminate the additional contact variables q and that these constraints are of index 1. The equations of motion of the wheelset are then derived by applying

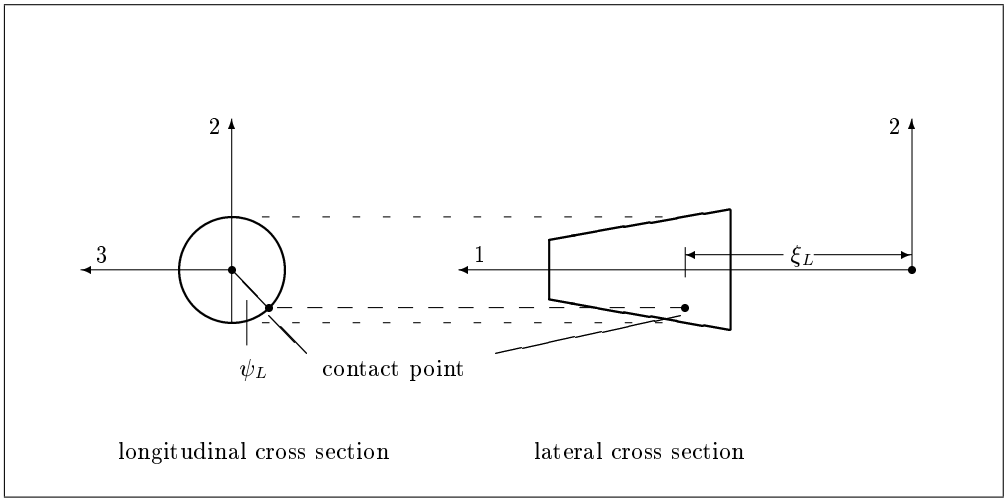

FIGURE II.22.3: *Shift angle and coordinate of contact point on the left side.*

the formalism of Newton and Euler. Here we used the property that this class of contact problems $(\partial g_1/\partial) q\, \dot{q} \equiv 0$. This also implies that if we, in order to get the index 2 formulation, differentiate the constraint (II.22.3) with respect to t, then we get

$$0 = \frac{\mathrm{d}g_1}{\mathrm{d}t}(p,q) = \frac{\partial g_1}{\partial p}\dot{p} + \frac{\partial g_1}{\partial q}\dot{q} = \frac{\partial g_1}{\partial p}\dot{p} - \frac{\partial g_1}{\partial q}\left(\frac{\partial g_2}{\partial q}\right)^{-1}\frac{\partial g_2}{\partial p}\dot{p},$$

which simplifies to (II.22.5).

Remarks

- $N(p,q,\lambda) \in \mathbb{R}^2$ denotes the normal forces which act in the contact points. They are necessary to evaluate the creep forces.
- The variable $\beta \in \mathbb{R}$ denotes the deviation of the angular velocity and is given by an additional differential equation.
- The parameters κ and α describe the track geometry. The setting $\kappa = \alpha = 0$ refers to a straight track.
- The constant C in (II.22.2) means that we internally scaled the Lagrange multipliers.

The initial values correspond to a setting in which the dynamic behavior of the wheelset model is investigated when the wheelset starts with an initial deflection in lateral direction (x-direction) of 0.14941 [cm]. In [Jas90], a limit cycle was observed for this problem and the model data given above. This type of limit cycle, the so-called hunting motion, is a well known phenomenon in railway vehicle dynamics. In Figure II.22.4 we see this limit cycle as computed by DASSL applied to the index-2 formulation of the problem. The results are in good agreement with those given in [Jas90], which were obtained by a state space form approach and with measurements on a hardware model.

22.4 Numerical solution of the problem

Tables II.22.2–II.22.3 present the reference solution at the end of the integration interval, and the run characteristics, respectively. Figure II.22.5 shows the the behavior of the components of p and the

TABLE II.22.2: *Reference solution at the end of the integration interval.*

u_1	$0.86355386965811 \cdot 10^{-2}$	u_{10}	$-0.13633468454173 \cdot 10^{-1}$
u_2	$0.13038281022727 \cdot 10^{-4}$	u_{11}	-0.24421377661131
u_3	$-0.93635784016818 \cdot 10^{-4}$	u_{12}	$-0.33666751972196 \cdot 10^{-3}$
u_4	$-0.13642299804033 \cdot 10^{-1}$	u_{13}	-0.15949425684022
u_5	$0.15292895005422 \cdot 10^{-2}$	u_{14}	$0.37839614386969 \cdot 10^{-3}$
u_6	$-0.76985374142666 \cdot 10^{-1}$	u_{15}	0.14173214964613
u_7	$-0.25151106429207 \cdot 10^{-3}$	u_{16}	$-0.10124044903201 \cdot 10^{-1}$
u_8	$0.20541188079539 \cdot 10^{-2}$	u_{17}	$-0.56285630573753 \cdot 10^{-2}$
u_9	-0.23904837703692		

TABLE II.22.3: *Run characteristics.*

solver	rtol	atol	h0	mescd	scd	steps	accept	#f	#Jac	#LU	CPU
DDASSL	10^{-4}	10^{-4}		1.35	0.15	5949	5117	10304	1407		0.3250
	10^{-5}	10^{-5}		2.78	1.40	9888	8667	16150	1815		0.4782
	10^{-6}	10^{-6}		3.67	2.32	16010	14298	25256	2577		0.7213
MEBDFI	10^{-4}	10^{-4}	10^{-4}	1.32	0.12	5758	5188	42694	1185	1185	0.4031
	10^{-5}	10^{-5}	10^{-5}	3.93	2.59	9317	8485	64945	1765	1765	0.6266
	10^{-6}	10^{-6}	10^{-6}	4.89	3.22	13240	12255	86260	2248	2248	0.8560
PSIDE-1	10^{-4}	10^{-4}		1.53	0.42	1276	945	22090	547	4920	0.5134
	10^{-5}	10^{-5}		2.81	1.67	2335	1507	39204	608	8752	0.8384
	10^{-6}	10^{-6}		4.52	3.34	3070	2068	54074	571	10736	1.0775

angular velocity β over the integration interval. Figures II.22.6- II.22.7 contain the work-precision diagrams. For this diagrams, we used: rtol $= 10^{-(4+m/8)}$, $m = 0, 1, \ldots, 48$; atol = rtol, h0 = rtol for MEBDFI. .

Remarks

- The Jacobian was computed internally by the solvers.
- For the runs with DASSL, we excluded the Lagrange multipliers from the error control by setting `atol(16)=atol(17)=rtol(16)=atol(17)=`10^{10}.
- The reference solution was computed using DASSL with atol = rtol $= 10^{-9}$ for p, v and q, and atol = rtol $= 10^{10}$ for λ.

References

[Jas87] A. Jaschinski. Anwendung der Kalkerschen Rollreibungstheorie zur dynamischen Simulation von Schienenfahrzeugen. Technical Report DFVLR 87-07, DFVLR Deutsche Forschungs- und Versuchsanstalt für Luft- und Raumfahrt, D-8031 Oberpfaffenhofen, 1987.

[Jas90] A. Jaschinski. *On the Application of Similarity Laws to a Scaled Railway Bogie Model*. PhD thesis, Technische Universiteit Delft, 1990.

[MM08] F. Mazzia and C. Magherini. *Test Set for Initial Value Problem Solvers, release 2.4*. Department of Mathematics, University of Bari and INdAM, Research Unit of Bari, February 2008. Available at http://www.dm.uniba.it/~testset.

[SFR91] B. Simeon, C. Führer, and P. Rentrop. Differential-algebraic equations in vehicle system dynamics. *Surv. Math. Ind.*, 1:1–37, 1991.

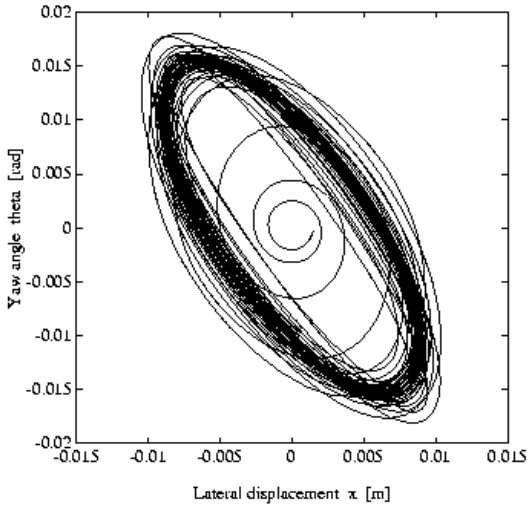

FIGURE II.22.4: *Limit cycle or 'hunting motion' of wheelset.*

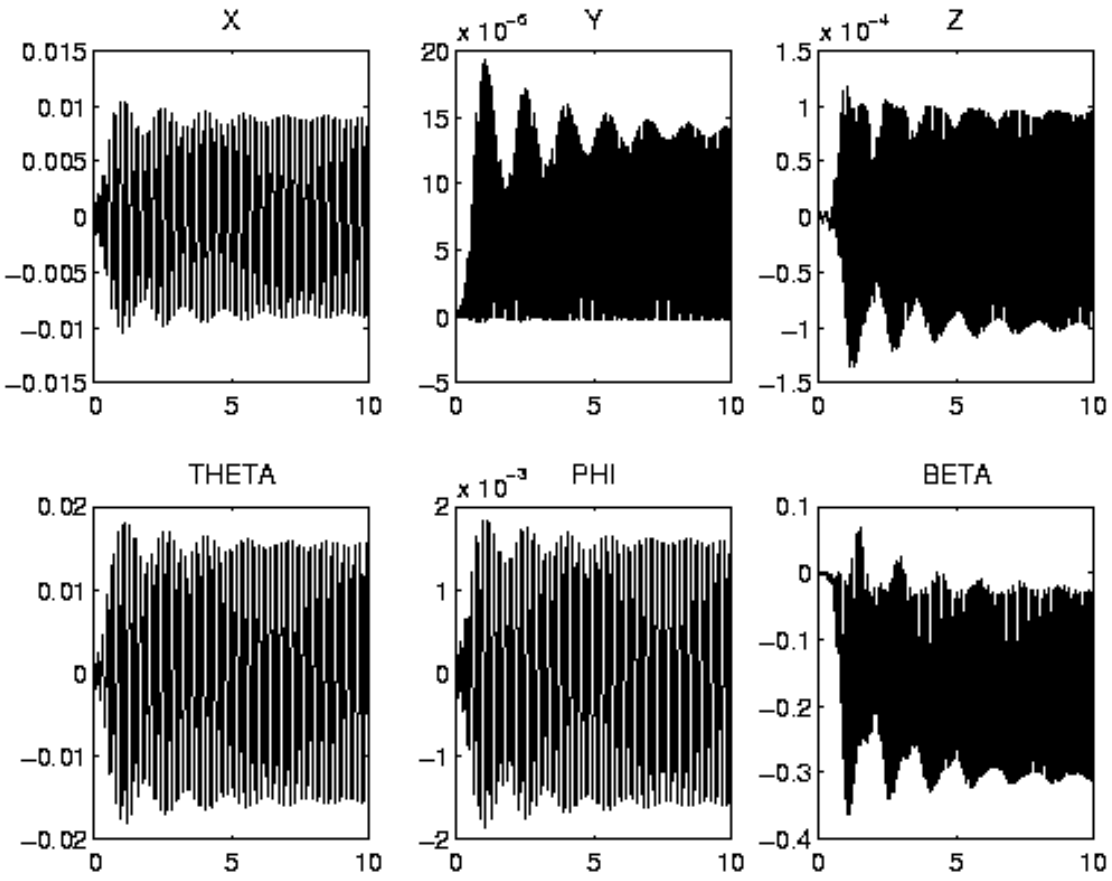

FIGURE II.22.5: *Behavior of some solution components over the integration interval.*

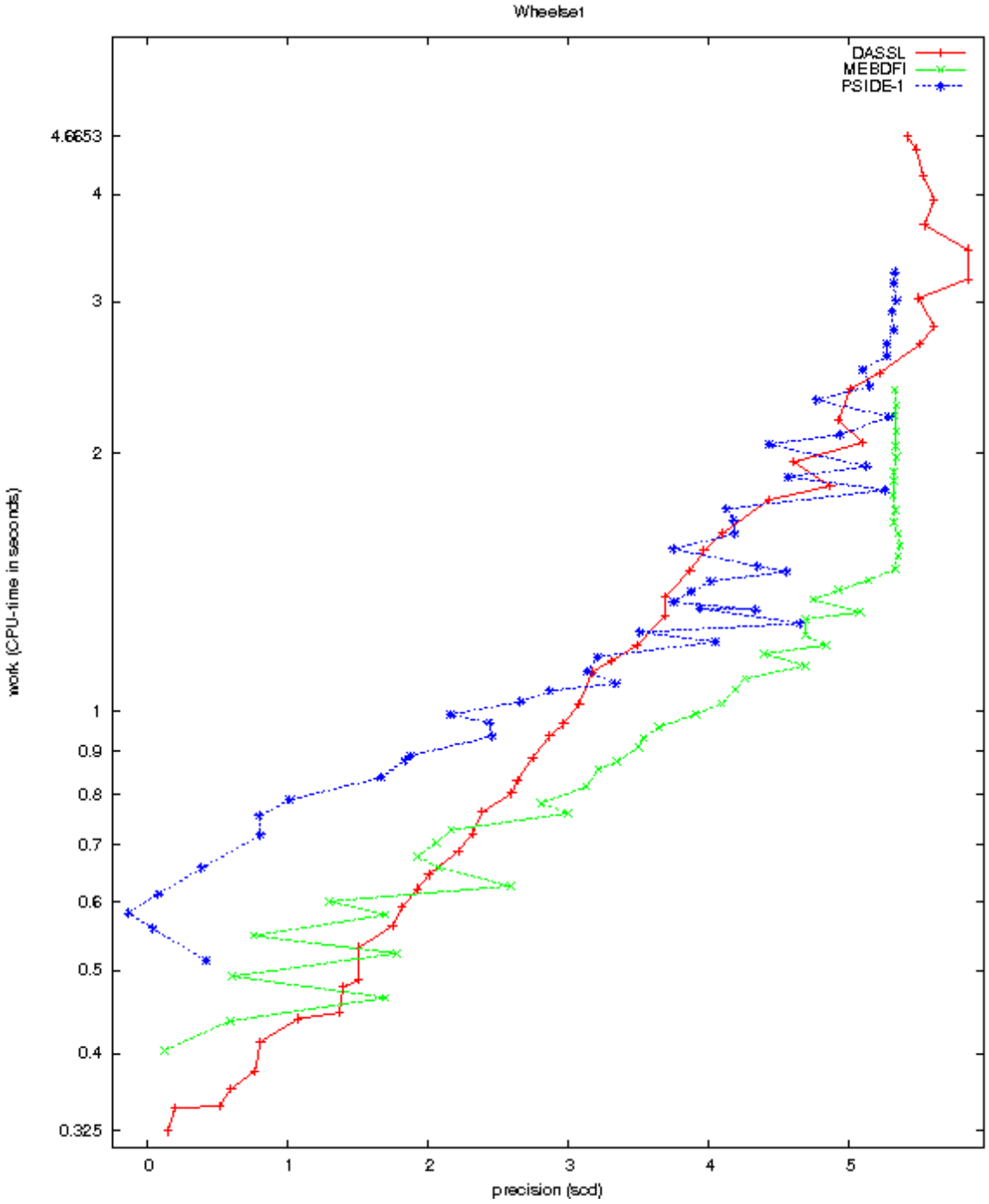

FIGURE II.22.6: *Work-precision diagram (scd versus CPU-time).*

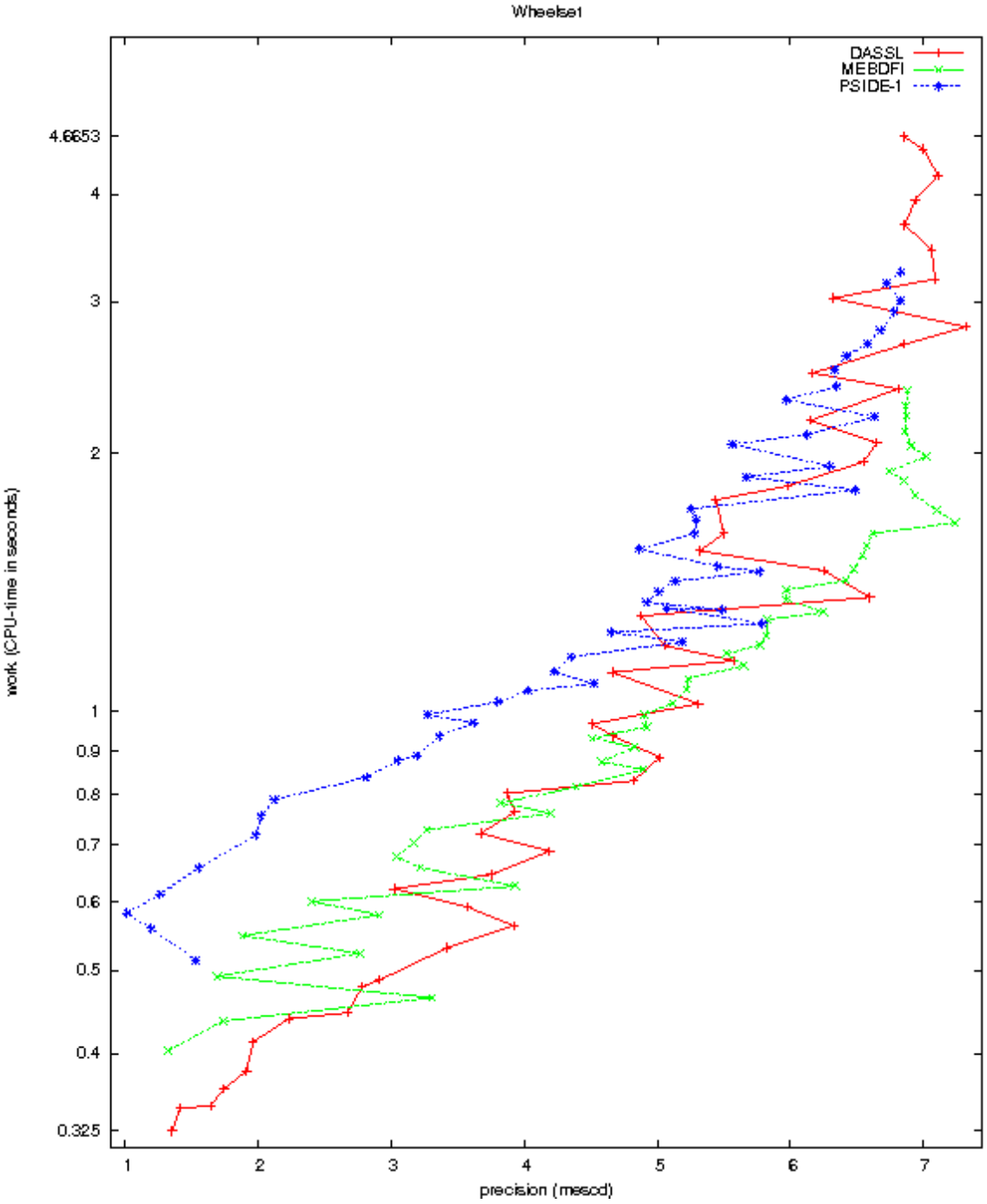

FIGURE II.22.7: *Work-precision diagram (mescd versus CPU-time).*